Controlling the transition between Turing and antispiral patterns by using time-delayed-feedback*

He Ya-Feng(贺亚峰), Liu Fu-Cheng(刘富成), Fan Wei-Li(范伟丽), and Dong Li-Fang(董丽芳)†

Hebei Key Laboratory of Optic-electronic Information Materials, College of Physical Science and Technology, Hebei University, Baoding 071002, *China*

(Received 24 July 2011; revised manuscript received 18 August 2011)

The controllable transition between Turing and antispiral patterns is studied by using a time-delayed-feedback strategy in a FitzHugh–Nagumo model. We treat the time delay as a perturbation and analyse the effect of the time delay on the Turing and Hopf instabilities near the Turing–Hopf codimension-two phase space. Numerical simulations show that the transition between the Turing patterns (hexagon, stripe, and honeycomb), the dual-mode antispiral, and the antispiral by applying appropriate feedback parameters. The dual-mode antispiral pattern originates from the competition between the Turing and Hopf instabilities. Our results have shown the flexibility of the time delay on controlling the pattern formations near the Turing–Hopf codimension-two phase space.

Keywords: pattern formation, Turing–Hopf bifurcations, time delay

PACS: 47.54.–r, 82.40.Ck, 82.40.Bj **DOI:** 10.1088/1674-1056/21/3/034701

1. Introduction

Spatiotemporal pattern formation has been extensively investigated in a variety of chemical, biological, and physical systems.[1] Since the observation of the Turing pattern and the spiral wave pattern in chlorite–iodide–malonic acid[2] and the Belousov–Zhabotinsky (BZ)[3] reaction, chemical reaction systems have attracted much attention in studies of pattern formation. In general, chemical systems can exhibit three types of properties: excitable, bistable, and Turing–Hopf. Some of these chemical reactions are light sensitive, such as the $Ru(bpy)_3^{2+}$ catalyst BZ reaction. The light-sensitive feature of the media makes it possible to control the spatiotemporal patterns by using certain strategies.[4] The control strategies can be classified into either external actions, such as periodical forcing,[5−11] or internal ones, such as time-delayed feedback.[12−16] Time-delayed feedback has been used widely due to its adaptive feature. For example, in an excitable system, the rigid rotation of a spiral can be stabilized by changing the domain diameter of feedback control.[13] In a bistable system, time-delayed feedback can control the nonequilibrium Ising–Bloch bifurcation, which realizes the transformation between spiral and labyrinth patterns.[14]

Turing–Hopf–type systems have shown interesting spatiotemporal patterns, such as hexagon, stripe, spiral, and antispiral patterns.[17,18] Some patterns are desirable, such as the Turing hexagon that grows in polystyrene film.[19] While some other patterns are avoided. Many methods have been attempted to control Turing and Hopf patterns. For example, time-delayed feedback with an appropriate intensity has been used to suppress or induce Turing patterns.[20] Recently, the systems near the Turing–Hopf codimension-two phase space have shown many fascinating patterns, such as the oscillatory Turing patterns obtained in a Brusselator model.[21−23] It is necessary to investigate the control of the spatiotemporal patterns near the Turing–Hopf codimension-two phase space. In this paper, we study the control of the transition between Turing and antispiral patterns by using a time-delayed-feedback strategy in a FitzHugh–Nagumo model. The effects of the time delay on the Turing and Hopf modes are analysed by treating the time delay as a perturbation. Numerical simulations show the flexibility of time-delayed feedback in controlling the transition between the Turing and antispiral patterns. We examine several dual-mode antispiral

*Project supported by the National Natural Science Foundation of China (Grant Nos. 10975043 and 10947166), the Natural Science Foundation of Hebei Province, China (Grant Nos. A2011201006 and A2010000185), and the Science Foundation of Hebei University.

†Corresponding author. E-mail: Donglf@hbu.edu.cn

© 2012 Chinese Physical Society and IOP Publishing Ltd

patterns and discuss their origins.

2. Model

This work is based on a delayed FitzHugh–Nagumo model expressed as

$$u_t = u - u^3 - v + D_u \nabla^2 u + F, \tag{1}$$

$$v_t = \varepsilon(u - a_1 v - a_0) + D_v \nabla^2 v + G, \tag{2}$$

where the time delay is applied with the forms

$$F = g_u(u(t-\tau) - u(t)), \tag{3}$$

$$G = g_v(v(t-\tau) - v(t)). \tag{4}$$

Here, variables u and v represent the concentrations of the activator and inhibitor, and D_u and D_v denote their diffusion coefficients, respectively. The small value ε characterizes the time scale of the two variables. The system described by Eqs. (1) and (2) can be either of Turing–Hopf, excitable or bistable type. In this paper, the parameter a_1 is chosen such that the system is of Turing–Hopf type. The parameter a_0 determines the position of the uniform steady states on the null lines of Eqs. (1) and (2). Unless otherwise specified, we choose $a_0 = 0$ such that the uniform steady states are $u_0 = v_0 = 0$. The parameters g_u and g_v are the feedback intensities of variables u and v, respectively. τ is the delayed time. In order to study the effect of the time delay on the Turing–Hop–type patterns, we first conduct linear stability analysis. In the analysis, we treat the delay as a perturbation by expanding the feedback terms in Eqs. (3) and (4) as

$$u(t-\tau) = u(t) - \tau \frac{\partial u(t)}{\partial t}, \tag{5}$$

$$v(t-\tau) = v(t) - \tau \frac{\partial v(t)}{\partial t}. \tag{6}$$

Thus, we obtain

$$(1 + \tau g_u) u_t = u - u^3 - v + D_u \nabla^2 u, \tag{7}$$

$$(1 + \tau g_v) v_t = \varepsilon(u - a_1 v - a_0) + D_v \nabla^2 v. \tag{8}$$

It can be seen that the terms of time are rescaled and determined by the delayed time and the feedback intensities. In the analysis, we fix the parameter $a_0 = 0$. So the uniform steady state of the system reads: $u_0 = v_0 = 0$. Then, we perturb the uniform steady state with a small spatiotemporal perturbation $(\delta u, \delta v) \sim \exp(\lambda t + \mathrm{i}\, kr)$, and obtain the following matrix equation for eigenvalues:

$$\begin{pmatrix} 1 & -1 \\ \varepsilon & -\varepsilon a_1 \end{pmatrix} \begin{pmatrix} \delta u \\ \delta v \end{pmatrix} = 0.$$

Thus we obtain the following quadratic equation for the eigenvalues

$$A\lambda^2 - B\lambda + C = 0, \tag{9}$$

where

$$A = (1 + \tau g_u)(1 + \tau g_v), \tag{10}$$

$$B = (1 + \tau g_u)(\varepsilon a_1 + k^2 D_v) - (1 + \tau g_v)(1 - k^2 D_u), \tag{11}$$

$$C = \varepsilon - (1 - k^2 D_u)(\varepsilon a_1 + k^2 D_v). \tag{12}$$

The dispersion relations $\lambda(k)$ of the system are defined by the roots of Eq. (9),

$$\lambda_{1,2} = \frac{B \pm \sqrt{B^2 - 4AC}}{2A}. \tag{13}$$

The positive real parts of $\lambda(k)$ give rise to Hopf instability and Turing instability, which occur at $k = 0$ and $k \neq 0$, respectively. In the absence of time delay, the stability diagram of the uniform steady state in the (a_1, ε) plane is shown in Fig. 1. The Turing bifurcation line (solid line) and the Hopf bifurcation line (dashed line) intersect at one point. Applying time delay will affect the two bifurcation lines. Here, we choose the parameters as (a_1, ε)=(0.5, 2) as indicated by the open circle in Fig. 1, which is beyond the Turing bifurcation line and is located on the Hopf bifurcation line. Our emphasis is on controlling the pattern formation by using the strategy of time-delayed feedback near the Turing–Hopf codimension-two phase space. In the following, we will discuss the effect of time delay on the Hopf and Turing instabilities, separately. Our analysis shows that the time delay affects both the Hopf and the Turing instabilities.

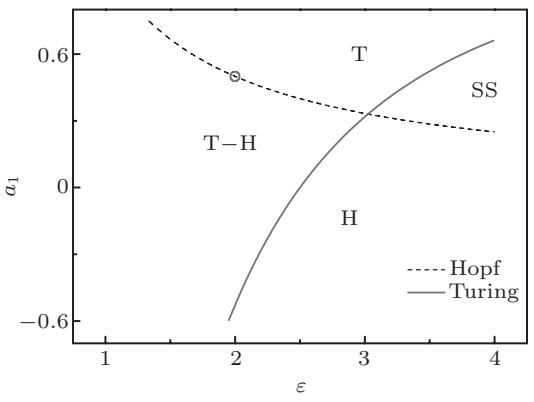


Fig. 1. Bifurcation diagram of the model system. Other parameters are: $D_u = 0.01$, $D_v = 0.1$, $a_0 = 0.0$, $\tau = 0.0$, $g_u = g_v = 0.0$.

The threshold of Hopf instability reduced from the linear stability analysis can be expressed as

$$a_1^{\mathrm{H}} = \frac{(1 + \tau g_v)}{\varepsilon(1 + \tau g_u)}, \tag{14}$$

and the corresponding oscillation frequency is

$$\omega_0 = \sqrt{\frac{\varepsilon}{(1+\tau g_u)(1+\tau g_v)} - \frac{1}{4}\left[\frac{\varepsilon a_1}{1+\tau g_v} + \frac{1}{1+\tau g_u}\right]^2}. \quad (15)$$

Equations (14) and (15) show that the strategy of time-delayed feedback plays an important role on controlling the bifurcation line and the oscillatory frequency of Hopf instability. It can be seen from Eq. (14) that applying a positive feedback to variable u (i.e., $g_u > 0$) and/or a negative feedback to variable v (i.e., $g_v < 0$) is functionally equivalent to increasing ε and/or decreasing a_1, and vise versa. We wish to mention that in a special case of $g_u = g_v$, the feedback no longer affects the bifurcation line of Hopf instability. However, it still changes the oscillatory frequency of the Hopf mode, as is expressed in Eq. (15). Figure 2(c) shows the dependence of the oscillatory frequency on the feedback intensities when applying feedback with identical intensities $g_u = g_v$. The oscillatory frequency decreases dramatically with feedback intensities. The stronger the intensities of the negative feedback are, the faster the Hopf mode oscillates. In the case of $g_u \neq g_v$, the dependences of the oscillatory frequency on the feedback intensities g_u and g_v are shown in Figs. 2(a) and 2(b), respectively. The solid line in Fig. 2 represents that the system is beyond the bifurcation line of Hopf instability. When the feedback g_u is applied individually, the oscillatory frequency increases from zero and then decreases with g_u as indicated by the solid line in Fig. 2(a). When the feedback g_v is applied individually, the oscillatory frequency decreases with g_v as shown in Fig. 2(b). Therefore, time-delayed feedback provides a way to change the oscillatory frequency of the Hopf mode even under the condition that the intensity of the Hopf mode remains unchanged.

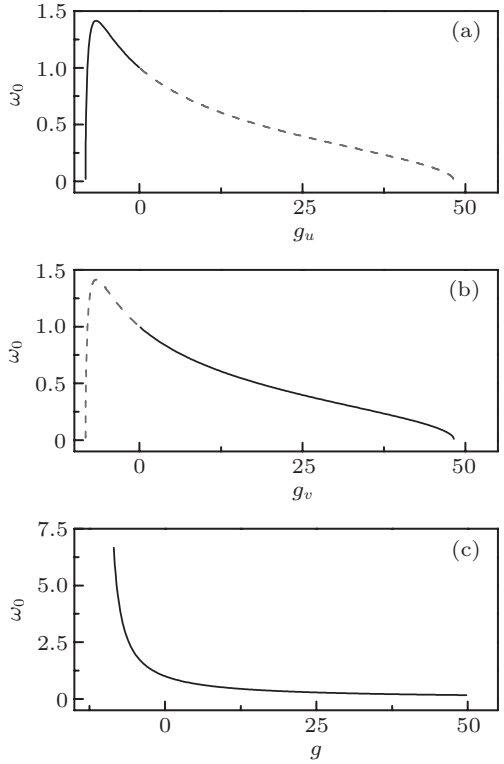


Fig. 2. Dependences of the oscillatory frequency of the Hopf mode on the feedback intensities in three cases: (a) $g_v = 0$, (b) $g_u = 0$, (c) $g_u = g_v = g$. Other parameters are: $D_u = 0.01$, $D_v = 0.1$, $a_1 = 0.5$, $a_0 = 0.0$, $\varepsilon = 2.0$, $\tau = 0.1$.

Figure 3 shows the dependence of the wave vector of the most unstable Turing mode on the feedback intensities. It can be seen that when the feedback g_u (g_v) is individually applied to the system, the wave vector increases (decreases) with the feedback intensity. This reveals that the wavelength of the Turing patterns can be controlled by using appropriate time-delayed feedback. In the special case of $g_u = g_v$, the time delay no longer affects the wave vector of the Turing mode, as indicated by the dashed line in Fig. 3. In this case, the time delay is equivalent to rescaled time, as shown in Eqs. (7) and (8), with the ratio of diffusion coefficients unchanged. Thus the wavelength of the Turing pattern is unaffected.

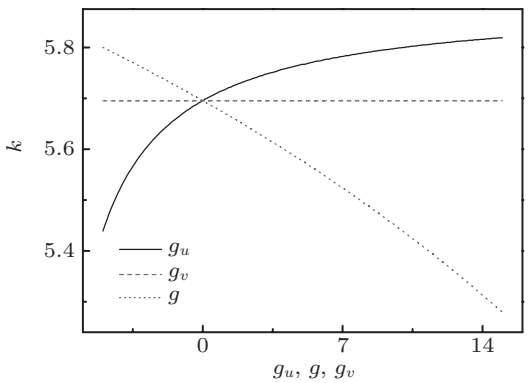


Fig. 3. Dependences of the wave vector of the most unstable Turing mode on the feedback intensities in three cases: solid line, $g_v = 0$; dashed line, $g_u = g_v = g$; dotted line, $g_u = 0$. Other parameters are: $D_u = 0.01$, $D_v = 0.1$, $a_1 = 0.5$, $a_0 = 0.0$, $\varepsilon = 2.0$, $\tau = 0.1$.

3. Two-dimensional numerical simulation

To illustrate the above analytical results about controlling pattern formation by using the strategy of

time-delayed feedback, we carry out a further numerical simulation in two dimensions. The grid sizes are 200×200, which represents domain sizes of 20×20 s.u., and the time step is $\Delta t = 0.01$ t.u.. The boundary condition is a zero flux boundary. In the above analysis, the time delay was treated as a perturbation, therefore the delayed time τ should be a small value. The feedback intensities g_u and g_v can be of any value. Equations (7) and (8) have shown that the delayed time τ and the feedback intensity g_u (g_v) are incorporated together, which means that the effect of a small delayed time and large feedback intensity, for example ($\tau = 0.1$, $g_u = 10.0$), is same as that of a large delayed time and small feedback intensity ($\tau = 10.0$, $g_u = 0.1$). In the following we show the numerical results only with small delayed time $\tau = 0.1$.

Figure 4 shows three cases for controlling the transition between Turing and antispiral patterns when the feedback g_v is individually applied to the system. In the case of $a_0 = -0.1$, Figs. 4(a)–4(d) show the transition from a hexagon pattern to an antispiral one with increasing g_v. When $g_v = 0.0$, it is a hexagon pattern as shown in Fig. 4(a). This is because the Turing mode is positive while the Hopf mode is negative, as illustrated in Fig. 5. With increasing feedback g_v, the Hopf mode becomes stronger and stronger, as shown in Fig. 5, which induces oscillating patterns such as the antispiral pattern. The Turing mode and the Hopf mode will compete with each other, which results in the coexistence of the stationary Turing pattern and the oscillating pattern, as shown in Fig. 4(b). If the Hopf mode is dominant, the oscillating pattern swallows the stationary Turing pattern gradually. If the Turing mode is prominent, the stationary Turing pattern will occupy the whole domain finally.

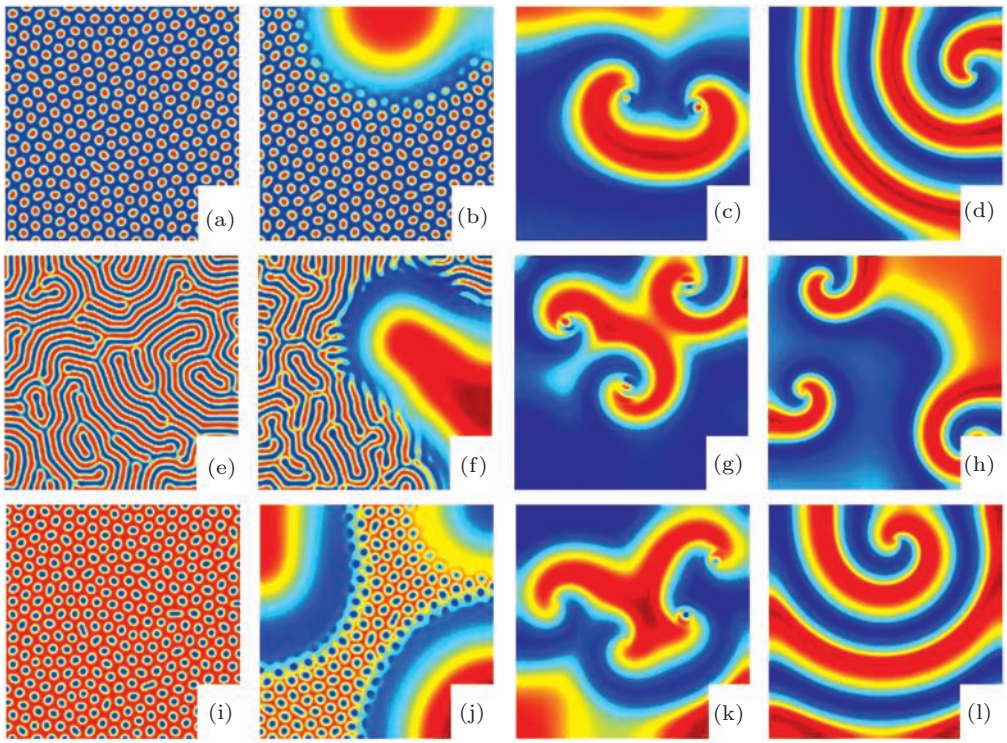


Fig. 4. (colour online) Transition from a Turing pattern to an antispiral pattern with increasing g_v in three cases: $a_0 = -0.1$, (a)–(d); $a_0 = 0.0$, (e)–(h); $a_0 = 0.1$, (i)–(l). The feedback intensities g_v in (a)–(d), (e)–(h), and (i)–(l) are 0.0, 5.0, 6.0, and 14.0, respectively. Other parameters are: $D_u = 0.01$, $D_v = 0.1$, $a_1 = 0.5$, $\varepsilon = 2.0$, $\tau = 0.1$, $g_u = 0.0$.

Figure 4(c) shows a dual-mode antispiral pattern, which exhibits the competition between the Hopf and Turing modes near the Turing–Hopf codimension-two phase space. The antispiral pattern originates from the negative dispersion $\mathrm{d}\omega/\mathrm{d}|k| < 0$ and the faster bulk oscillation $\omega_0 > \omega_k$ as indicated by the dashed lines in Fig. 5. Here, we focus on the core region of the antispiral pattern. As is well known, the tip of the oscillating antispiral is due to a topological defect, and the amplitude near the tip is zero. However, in the present case of competition between the Hopf and Turing instabilities, the amplitude near the tip is not

yet zero. The core of the antispiral pattern contains stationary hexagonal spots originating from the Turing instability, as shown in Fig. 4(c). The wavelength of the hexagon pattern near the core is about 1.1 s.u. which corresponds to the wave vector of the most unstable Turing mode $k = 5.7$. It can be seen from Fig. 6 that the amplitude of the hexagon pattern is lower than that of the antispiral patten. Far from the core region, the hexagon pattern is damped by the Hopf oscillation. This is similar to the dual-mode spirals observed by Mau[24] and Kepper.[25] With g_v increasing, the amplitude of the antispiral pattern increases gradually. The hexagon spots near the core are suppressed by the large amplitude oscillation. The core of the antispiral pattern returns to normal, as shown in Fig. 4(d).

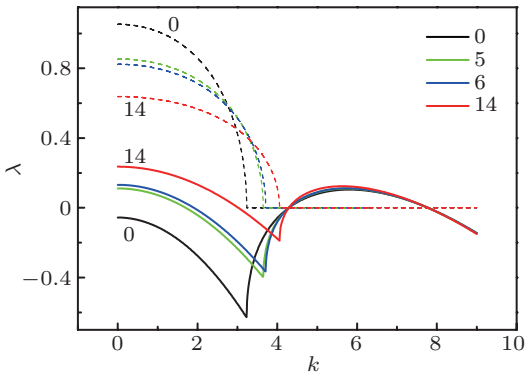


Fig. 5. (colour online) Dispersion relation of the delayed model in four cases: $g_v = 0$, 5, 6, 14. The solid (dashed) lines represent the real (imaginary) part of the eigenvalue. The numbers label represent the values of g_v. Other parameters are: $D_u = 0.01$, $D_v = 0.1$, $a_1 = 0.5$, $a_0 = -0.1$, $\varepsilon = 2.0$, $\tau = 0.1$, $g_u = 0.0$.

In the case of $a_0 = 0.0$, Figs. 4(e)–4(h) show the transition from the stripe to antispiral patterns with increasing g_v. This progress is similar to the aforementioned transition. The core of this dual-mode antispiral contains a stripe pattern, as shown in Fig. 4(g). In the case of $a_0 = 0.1$, Figs. 4(i)–4(l) show the transition from the honeycomb to antispiral patterns with increasing g_v. The core of this dual-mode antispiral contains a honeycomb pattern, as shown in Fig. 4(k). In other words, we can control the transition between the Turing and antispiral patterns by using time-delayed feedback.

The dual-mode antispiral is similar to the observation by Yuan *et al.*[26] in a CIMA reaction. They called it a Turing–Hopf mixed state and attributed its formation to the 3D effect of the reaction medium, where the Turing pattern and the antispiral pattern occur in different places in the third dimension. However, in our case the dual-mode antispiral pattern occurs during the transition with g_v increasing. In this progress the Hopf mode becomes stronger and stronger, and the amplitude of the antispiral pattern increases gradually. When the amplitudes of the Turing pattern and the antispiral pattern are comparable as indicated in Fig. 5, the Turing pattern remains near the core of the antispiral pattern, which forms a dual-mode antispiral pattern, as shown in Figs. 4(c), 4(g), and 4(k). Far from the core region, the Turing pattern is damped by the Hopf oscillation. With g_v increasing continuously, the Hopf mode becomes stronger. The amplitude of the antispiral pattern is much larger than that of the Turing pattern. The Turing patterns are nearly damped in the whole domain. Thus we observe the normal antispiral patterns shown in Figs. 4(d), 4(h), and 4(l).

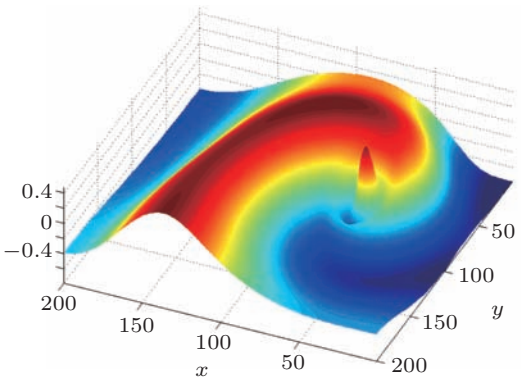


Fig. 6. (colour online) Surface plot of the core of a dual-mode antispiral pattern. The amplitude of the hexagonal spots near the core is lower than that of the antispiral pattern. The parameters are the same as that in Fig. 4(c).

In the above simulations, we have shown the controllable transition between the Turing patterns and the antispiral pattern by increasing the feedback intensity g_v. As illustrated in Eq. (14), the effect of increasing g_v is equivalent to that of decreasing g_u. The aforementioned transition from the Turing patterns (hexagon, stripe, and honeycomb) to the antispiral pattern can be reproduced by decreasing feedback g_u. This has been confirmed by extensive numerical simulations (not shown here). Therefore, time-delayed feedback provides a flexible strategy to control the Turing and antispiral patterns near the Turing–Hopf codimension-two phase space.

4. Conclusion

We have studied the transition between Turing and antispiral patterns, which is controlled by time-delayed feedback in a delayed FitzHugh–Nagumo model. We treated the time delay as a perturbation and analysed the effect of the time delay on the Turing and Hopf instabilities near the Turing–Hopf codimension-two phase space. The time delay affects the wave vector of the Turing mode and the oscillation frequency of the Hopf mode. Analyses show that the effect of a small delay time and large feedback intensity on the system is equivalent to that of a large delay time and a small feedback intensity. Time-delayed feedback provides a flexible way to control pattern formation. The transition between the Turing patterns (hexagon, stripe, and honeycomb), the dual-mode antispiral, and the antispiral is numerically studied by using appropriate feedback parameters. The dual-mode antispiral patterns originate from the competition between the Turing and Hopf modes. Our results could contribute to the control of pattern formations in light-sensitive BZ or chlorine dioxide–iodine–malonic acid chemical reactions.

References

[1] Cross C C and Hohenberg P C 1993 *Rev. Mod. Phys.* **65** 851

[2] Ouyang Q and Swinney H L 1991 *Nature* **352** 610

[3] Zaikin A N and Zhabotinsky A M 1970 *Nature* **225** 535

[4] Guo W Q, Qiao C, Zhang Z M, Ouyang Q and Wang H L 2010 *Phys. Rev.* E **81** 056214

[5] Mikhailov A S and Showalter K 2006 *Phys. Rep.* **425** 79

[6] Luo J M and Zhan M 2010 *Phys. Rev.* E **78** 016214

[7] Chen J X, Xu J R, Yuan X P and Ying H P 2009 *J. Phys. Chem.* B **113** 849

[8] Zhang H, Cao Z J, Wu N J, Ying H P and Hu G 2005 *Phys. Rev. Lett.* **94** 188301

[9] Cui X H, Huang X Q, Cao Z J, Zhang H and Hu G 2008 *Phys. Rev.* E **78** 026202

[10] Tang G N, Deng M Y, Hu B and Hu G 2008 *Phys. Rev.* E **77** 046217

[11] Ma J, Jia Y, Yi M, Tang J and Xia Y F 2009 *Chaos, Solitons Fractals* **41** 1331

[12] Schneider F M, Schöll E and Dahlem M A 2009 *Chaos* **19** 015110

[13] Kheowan O U, Zykov V S and Müller S C 2002 *Phys. Chem. Chem. Phys.* **4** 1334

[14] He Y F, Ai B Q and Hu B B 2010 *J. Chem. Phys.* **133** 114507

[15] Hu H X, Li Q S and Li S 2007 *Chem. Phys. Lett.* **447** 364

[16] Golovin A A, Kanevsky Y and Nepomnyashchy A A 2009 *Phys. Rev.* E **79** 046218

[17] Wang W M, Liu H Y, Cai Y L and Li Z Q 2011 *Chin. Phys.* B **20** 074702

[18] Li H H, Xiao J H, Hu G and Hu B B 2010 *Chin. Phys.* B **19** 050516

[19] Gotoh H, Kamada H, Saitoh T, Shigemori S and Temmyo J 2004 *Appl. Phys. Lett.* **85** 2836

[20] Li Q S and Ji L 2004 *Phys. Rev.* E **69** 046205

[21] Yang L F, Dolnik M, Zhabotinsky A M and Epstein I R 2002 *Phys. Rev. Lett.* **88** 208303

[22] Ricard M R and Mischler S 2009 *J. Nonlinear Sci.* **19** 1432

[23] Yang L F, Zhabotinsky A M and Epstein I R 2004 *Phys. Rev. Lett.* **92** 198303

[24] Mau Y, Hagberg A and Meron E 2009 *Phys. Rev.* E **80** 065203(R)

[25] de Kepper P, Perraud J J, Rudovics B and Dulos E 1994 *Int. J. Bifurcation and Chaos* **4** 1215

[26] Yuan X J, Shao X, Liao H M and Ouyang Q 2009 *Chin. Phys. Lett.* **26** 024702